Human Cancer Biology

Clinical Cancer Research

A Noncanonical Flt3ITD/NF-κB Signaling Pathway Represses *DAPK1* in Acute Myeloid Leukemia

Rajasubramaniam Shanmugam[1,4], Padmaja Gade[5], Annique Wilson-Weekes[1,4], Hamid Sayar[1], Attaya Suvannasankha[1,4], Chirayu Goswami[2], Lang Li[2], Sushil Gupta[1], Angelo A. Cardoso[1], Tareq Al Baghdadi[1], Katie J. Sargent[3], Larry D. Cripe[1], Dhananjaya V. Kalvakolanu[5], and H. Scott Boswell[1,4]

Abstract

Purpose: Death-associated protein kinase 1 (DAPK1), a tumor suppressor, is a rate-limiting effector in an endoplasmic reticulum (ER) stress-dependent apoptotic pathway. Its expression is epigenetically suppressed in several tumors. A mechanistic basis for epigenetic/transcriptional repression of *DAPK1* was investigated in certain forms of acute myeloid leukemia (AML) with poor prognosis, which lacked ER stress-induced apoptosis.

Experimental Design: Heterogeneous primary AMLs were screened to identify a subgroup with Flt3ITD in which repression of *DAPK1*, among NF-κB–and *c*-Jun–responsive genes, was studied. RNA interference knockdown studies were carried out in an Flt3ITD$^+$ cell line, MV-4-11, to establish genetic epistasis in the pathway Flt3ITD–TAK1–DAPK1 repression, and chromatin immunoprecipitations were carried out to identify proximate effector proteins, including TAK1-activated p52NF-κB, at the *DAPK1* locus.

Results: AMLs characterized by normal karyotype with Flt3ITD were found to have 10- to 100-fold lower *DAPK1* transcripts normalized to the expression of *c*-Jun, a transcriptional activator of *DAPK1*, as compared with a heterogeneous cytogenetic category. In addition, *Meis1*, a *c*-Jun-responsive adverse AML prognostic gene signature was measured as control. These Flt3ITD$^+$ AMLs overexpress relB, a transcriptional repressor, which forms active heterodimers with p52NF-κB. Chromatin immunoprecipitation assays identified p52NF-κB binding to the *DAPK1* promoter together with histone deacetylase 2 (HDAC2) and HDAC6 in the Flt3ITD$^+$ human AML cell line MV-4-11. Knockdown of p52NF-κB or its upstream regulator, NF-κB–inducing kinase (NIK), de-repressed *DAPK1*. *DAPK1*-repressed primary Flt3ITD$^+$ AMLs had selective nuclear activation of p52NF-κB.

Conclusions: Flt3ITD promotes a noncanonical pathway *via* TAK1 and p52NF-κB to suppress DAPK1 in association with HDACs, which explains *DAPK1* repression in Flt3ITD$^+$ AML. *Clin Cancer Res; 18(2); 360–9. ©2011 AACR.*

Introduction

Recent evidence indicates that attenuation of the unfolded protein response (UPR)—an endoplasmic reticulum (ER)–dependent stress response—may explain therapeutic failure of acute myeloid leukemia (AML; refs. 1–3). Downstream transcriptional mediators of the Flt3 internal tandem duplication (ITD) in AML may impose such a status by regulating expression of effectors that control stress-dependent apoptosis. For example, the ratio of ER levels of bcl-2 versus death-associated protein kinase 1 (DAPK1) as well as other effectors may determine this output at a defined set-point (4–6).

DAPK1 is a calcium-calmodulin–dependent serine–threonine protein kinase, which suppresses tumor cell survival and metastasis via autophagy and apoptosis. It plays a central role in ER stress–dependent apoptosis (7). *DAPK1* expression is affected by a variety of oncogenic signals (7, 8). We previously showed the existence of a Flt3–JNK1–*c*-Jun

Authors' Affiliations: Departments of [1]Medicine (Hematology/Oncology Division) and [2]Biostatistics and Computational Biology, Indiana University Melvin and Bren Simon Cancer Center, Indiana University School of Medicine; [3]Indiana University Health Systems; [4]Veterans Affairs Medical Center, Indianapolis, Indiana; and [5]Department of Microbiology and Immunology, Greenebaum Cancer Center, University of Maryland School of Medicine, Baltimore, Maryland

Note: Supplementary data for this article are available at Clinical Cancer Research Online (http://clincancerres.aacrjournals.org/).

Current address for R. Shanmugam: Regional Medical Center (ICMR), Jabalpur, India

P. Gade and A. Wilson-Weekes contributed equally to this work.

Corresponding Author: H. Scott Boswell, Indiana University Melvin and Bren Simon Cancer Center, R3-C-312, 980 W. Walnut Street, Indianapolis, IN 46202. Phone: 317-274-0528; Fax: 317-274-0396; E-mail: hboswell@iupui.edu

doi: 10.1158/1078-0432.CCR-10-3022

Translational Relevance

Acute myeloid leukemia (AML) is a group of complex and heterogeneous diseases, which can be classified according to cytogenetic/genotypic features of the blast cells and activated signaling pathways. These signaling pathways cooperate to promote blast cell survival and to prevent tumor suppressor-induced senescence. In this article, we report a tyrosine kinase (Flt3ITD)-initiated noncanonical NF-κB signaling pathway in a subset of AMLs, where p52NF-κB, in association with certain histone deacetylases (HDAC), represses the tumor suppressor gene *DAPK1*. DAPK1 is an essential player in endoplasmic reticulum (ER)–stress-induced apoptosis, and is implicated in poor outcome of AML by its repression. The mechanism for repression of DAPK1 by p52NF-κB and HDACs, influenced by Flt3ITD, was found to involve the MAP3K, TAK1. Because TAK1 is one among the most highly expressed genes in a leukemic stem cell signature for poor-risk AML, these studies focus attention on the interface between signal transduction and epigenetic remodeling in AML.

pathway in Flt3ITD$^+$ AML (9). *c*-Jun is known to drive the expression of not only *bcl-2*, but also *DAPK1* (10, 11). However, the latter circumstance would be antagonistic to the progression of poor-prognosis Flt3ITD$^+$ AML. On the other hand, NF-κB and CRE/*c*-Jun regulatory sites coexist on the promoters of certain tumor suppressor or cytokine genes including *DAPK1*, and the importance of NF-κB signaling in AML is known (12–15). We hypothesized that a resistance to apoptosis in certain AMLs occurs via severe repression of *DAPK1*, through recruitment of p52NF-κB to the putative NF-κB site at −134bp of its promoter (12, 13). Indeed, expression of DAPK1 is lost in a number of human cancers, including leukemias (16). Although epigenetic suppression of *DAPK1* is well reported, the upstream mechanisms that contribute to tumor promotion via the recruitment of epigenetic apparatus to the *DAPK1* promoter are not defined (16–19).

We hypothesized that tandem activation of both *c*-Jun N-terminal kinase 1 (JNK1) and IκB kinase (IKK)/NF-κB may be involved in concerted regulation of antiapoptotic as well as proapoptotic genes to achieve an antiapoptotic/proapoptotic effector balance (e.g., bcl-2/DAPK1) to permit higher aggressiveness in Flt3ITD$^+$ AML (4, 6, 14, 20). This postulation was tested in context of prior functional and cohort analyses of AML blasts carried out in our laboratory that linked Flt3 phosphorylation/activation to JNK1 phosphorylation (9) and with regard to the known role for *c*-Jun1/AP-1 in *DAPK1* and *bcl-2* expression (10, 11). In addition, we inferred that a conserved dual-activation mechanism, which relies upon TAK1, for JNK1–*c*-Jun and IKK–NF-κB may exist (21) to promote the optimal antiapoptotic/proapoptotic effector balance. This hypothesis was given emphasis by the recognition that *TAK1* is among the most highly expressed genes in a leukemic stem cell (LSC) signature of poor-risk AML in which *DAPK1* repression coexists (22, 23).

In this study, we showed that TAK1 activated p52NF-κB, binds at the tandem NF-κB and CRE sites of *DAPK1*, and recruits certain transcriptional repressors, belonging to the histone deacetylase (HDAC) family (12). Because p52NF-κB is a downstream target of Flt3 signaling, we hypothesized that interruption of this signaling arm of Flt3 would result in a de-repression of *DAPK1* to contribute toward enhanced apoptosis in Flt3 ITD$^+$ AMLs. Finally, we propose a therapeutic model for the rational combination of Flt3- and HDAC-inhibitors for suppressing AML growth.

Materials and Methods

Cell culture

The human leukemic cell lines, HL-60 and MV-4-11 (derived from a biphenotypic leukemia), were obtained from the American Type Culture Collection (ATCC) in McCoy's and RPMI media, respectively, supplemented with 10% fetal calf serum. The MV-4-11 cell line overexpresses Flt3-ITD and harbors the 11q23 translocation [t(4)] involving the *MLL* gene (9). Blast cells from the bone marrow of patients with AML were obtained at the time of diagnosis, after informed consent. The buoyant fraction was isolated over Ficoll–Hypaque, and then washed with PBS before processing. The cohort of AMLs subjected to gene expression analysis showed mean 88 ± 10% blasts (Supplementary Table S1). Cells were lysed and fractionated into nuclear and cytoplasmic fractions using the NE-PER Extraction Kit (Pierce Biotechnology). For Western blot analysis, bone marrow samples with ≥70% blast cells in the purified aspirate were used.

Transfections and reporter assays

MV-4-11 cells were electroporated using the Amaxa system and then placed in McCoy's medium supplemented with 10% FBS. Cells were transfected with a luciferase reporter (13) driven by the *DAPK1* promoter (1.2 κB) harboring either wild-type or mutated CRE site (−177 bp). Wild-type *c*-Jun or vector control was co-transfected in some experiments with the *DAPK1* reporter. *Renilla* luciferase was cotransfected to normalize for variations in transfection efficiency.

Western blot analysis

Cytosolic or nuclear proteins were subjected to Western blotting with indicated antibodies as described previously (9). Densitometry was carried out to quantify specific bands, and data were normalized to either cytoplasmic glyceraldehyde-3-phosphate dehydrogenase (GAPDH) or nuclear (Sp1) internal controls, depending on the case.

Chromatin immunoprecipitation assay

Chromatin immunoprecipitation (ChIP) assays were conducted as previously described (13). In brief, DNA–protein complexes were cross-linked by incubating

5×10^7 cells with 1% formaldehyde. After washing, cells were lysed and chromatin was sheared to yield DNA fragments (~800 bp) using a Branson Digital Sonifier. The lysate was then centrifuged, and soluble chromatin was immunoprecipitated with 5 μg of the indicated antibody. The protein–DNA complexes were collected after incubating with protein-A magnetic beads, washed, and reverse cross-linked by heating at 65°C overnight using 1% SDS and 0.1 mol/L NaHCO3. DNA released from the complexes was purified using the QIAquick Spin Kit (Qiagen, Inc) and collected. The purified DNA samples from the input, immunoprecipitated with either a nonspecific immunoglobulin G (IgG; control) or specific IgG (experimental), were subjected to either PCR or quantitative PCR (qPCR) analyses with *DAPK1* promoter specific primers: 5′-AGTCCTCAGAAATCTC ATGCAAG-3′ and 5′-CATTAGAGTCCAAGACAGTA-3′. DNA extracted from soluble chromatin was used as an input control for each reaction. Each experiment was repeated at least 3 independent times with multiple samples ($n = 4$) for ensuring the consistency of the results.

Real-time reverse transcriptase PCR analysis in a gene-set enrichment array panel

Total RNAs from blood/bone marrow specimens were isolated using the RNeasy Kit (Qiagen, MD) according to the manufacturer's instructions. Total RNA (500 ng) from each specimen was converted to cDNA using the Superscript III First strand cDNA Synthesis Kit (Invitrogen). Relative gene expression was quantified using TaqMan Gene Expression Assays (Applied Biosystems) and ABI PRISM 7900 real-time PCR machine. Quantitative reverse transcriptase (qRT-PCR) for 31 AML associated genes and 1 housekeeping gene was carried out at low-density array (LDA) format according to the manufacturer's protocol (TaqMan Gene Expression Micro Fluidic card, 4346799; Applied Biosystems). The amount of cDNA per card was 200 ng. 18S rRNA was chosen as an internal control. Relative expression was calculated using RQ manager Ver 1.2 (Applied Biosystems) using a 1-patient volunteer sample (CBF^+, very low *c*-Jun and negative for Flt3ITD and Meis-1 expression) as a calibrator. Copy number or fold-change in expression was calculated using the $2^{-\Delta\Delta Ct}$ method (24).

Statistical analyses

Individual patient gene expression data within the defined cohorts was subjected to statistical analysis using the Mann–Whitney/Wilcox test and a P value <0.05 was considered significant.

Results

Flt3ITD signaling is associated with loss of DAPK1 protein expression

Bcl-2 and *DAPK1* are targets of transcriptionally active *p*-Jun, and are potentially relevant to the pathogenesis of Flt3ITD AML (10, 11). However, optimal progression of Flt3ITD-driven AML would be served by repression of *DAPK1* with simultaneously overexpressed bcl-2, whose transcription is critically dependent on a CRE/*c*-Jun site (25).

We postulated that the poor prognosis of Flt3ITD AMLs may relate to a lack of *DAPK1* expression, dependent on a transcriptional milieu affecting the tandem CRE and κB elements of its promoter, thus distinguishing *DAPK1* regulation in $Flt3ITD^+$ versus $Flt3ITD^-$ AML. Expression of DAPK1 in $Flt3ITD^+$ AML may be selectively blocked by a p52NF-κB/HDAC-associated complex at the κB/CRE site (12). Both NF-κB and *c*-Jun can be generated by activation mechanisms (IKK and JNK1) regulated by the MAP3K, TAK1, respectively (21).

Moreover, analysis of AML blasts separated by their Flt3ITD status, in chronologic succession, showed an apparent relationship with expression of phospho-*c*-Jun and TAK1 activation, through phosphorylation (Fig. 1A and B; and data not shown). Interestingly, in an $Flt3ITD^+$ sample (#2797) with very high pTAK1/*p*-Jun activity, the lowest expression of *DAPK1* was observed, when compared with 2 other AMLs lacking the Flt3ITD mutation (Fig. 1A). This is contrary to the expectation based on the known role for *c*-Jun and its transcriptional partner canonical NF-κB on *DAPK1* expression (refs. 11, 13, 15; and see below), and expression levels of *p*-Jun were quite similar in $Flt3ITD^-$ AML #2993 (normal karyotype) with high DAPK1, compared with $NKFlt3ITD^+$ 2797 (Fig. 1A).

To further explore the role of Flt3ITD/TAK1 in promoting cooperation between *p*-Jun and NF-κB species, a series of AML blasts characterized by normal karyotype with Flt3-ITD (NK-Flt3ITD) was studied for *c*-Jun phosphorylation and TAK1 activation. We found that, like the positive control cell line MV-4-11, the normal karyotype $Flt3ITD^+$ patient blasts express significant levels of Flt3 protein, active/total TAK1, and *p*-Jun (Fig. 1). In one of the AML blasts (#2857), treatment with Flt3-ligand *ex vivo* led to downregulation of Flt3, followed by transient upregulation of phospho-TAK1 and DAPK1 levels, which returned to baseline (Fig. 1B). Indeed, *DAPK1*-Luc reporter analyses in MV-4-11 revealed abundant activity, and exogenous *c*-Jun could significantly augment luciferase expression by 2-fold ($P < 0.004$). However, a mutant promoter lacking the CRE site had blunted activity. RNA interference (RNAi) with Flt3 and JNK1 showed that interference with the Flt3–JNK1 axis inhibited *DAPK1* and *bcl-2* expression (Fig. 1C).

On the other hand, Western blot analyses for DAPK1 expression in relation to *p*-Jun, showed widely varied expression of DAPK1 between blast samples, contrary to expectation if only *p*-Jun were the regulatory determinant (Fig. 1B). All $Flt3ITD^+$ samples, except #2841, had an extremely low (#2857) or barely detectable DAPK1 expression (#2797, 2854), similar to that observed in MV-4-11—where DAPK1 was undetectable (Fig. 1). This was noted in spite of high and largely invariant levels of *p*-Jun (Fig. 1). Furthermore, the occurrence of highest bcl-2 levels in #2797 primary AML blasts with lowest DAPK1 was contrary to expectation and quite similar to the situation in MV-4-11 (Fig. 1).

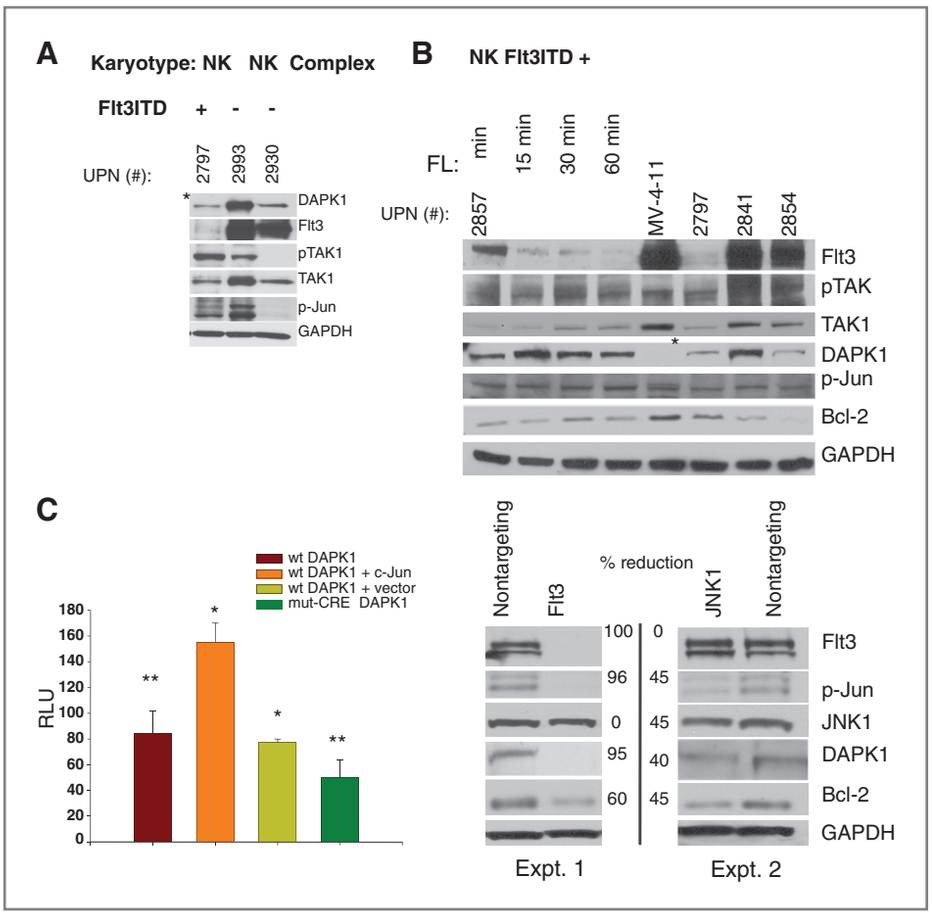

Figure 1. Downregulation of DAPK1 expression in the MV-4-11 cell line that bears Flt3ITD, and series of primary AML blasts with normal karyotypes (NK) and Flt3ITD, as compared with *FltITD*$^-$ AMLs. Western blot analyses were conducted. A, Flt3ITD$^+$ AML 2797 and FltITD$^-$ AMLs #2930 and 2993 showed correlation of TAK1 phosphorylation levels with phosphorylation status of the secondary (TAK1-JNK1) downstream transcription factor target *c*-Jun. In addition, *DAPK1* (a *c*-Jun target gene) levels were analyzed in these samples: lower expression levels were found in the Flt3ITD$^+$ AML 2797 (denoted in 2 places by asterisks; 1.5-fold and >6-fold reduction) with strong TAK1 activation, when compared with FltITD$^-$ AMLs #2930 and 2993, respectively. B, DAPK1 levels were quantified densitometrically in Flt3ITD$^+$ AMLs and MV-4-11 cell line (for #2841, 3- to 4-fold higher than 2797 and 2854, respectively, as well as 1.5-fold higher vs. 2857). C, *DAPK1* promoter activity is significantly augmented 2-fold by *c*-Jun (*, $P < 0.004$) in MV-4-11 cells. *DAPK1* promoter vector with a mutated CRE site showed decreased activity (**, $P < 0.03$). Data represent mean ± SE replicate determinations, from 3 experiments. Results of Western blotting of MV-4-11 cells treated with RNAi for Flt3 or JNK1, compared with nontargeting control siRNA. Knockdown of Flt3ITD reduces *p*-jun activation (by 96%) and DAPK1 and bcl-2 expression by 95% and 60%, respectively. RNAi-mediated knockdown of JNK1 (45%) reduces *p*-jun levels by 45% and DAPK1 and bcl-2 levels by 40% and 45%, respectively. RLU, relative luciferase units; UPN, Unique Patient Number.

We next pursued the clinical/biologic significance of these findings in MV-4-11 and in a larger series of NKFlt3ITD$^+$ samples. Genome-wide gene expression profiling coupled with real-time RT-PCR was carried out using AML blasts from patients with defined cytogenetic and molecular Flt3ITD status from 3 distinct cohorts: (i) normal karyotype Flt3ITD; (ii) tMLL-AML; and (iii) other genotypic/cytogenetic alterations, including those with monosomy 5/7 and a complex karyotype. These analyses included the cohort of blasts from the normal karyotype of patients with Flt3ITD AML (Fig. 1). We studied the expression of *DAPK1*, because it is responsive to *c*-Jun/AP-1 and (p65) canonical NF-κB, to examine the basis for gene repression guided by p52NF-κB in the absence of p65NF-κB. In such circumstance, p52NF-κB heterodimers with relB could recruit transcriptional co-repressors (12,14, 26, 27). In addition to *c-jun and relB* (26), expression of another *c*-Jun target gene *meis1* (11) was analyzed as a positive control in real-time RT-PCR.

Compared with CBF$^+$ AML or PML-RAR$^+$ AML (which express low *c*-Jun and which fail to express hoxA9/meis1; data not shown; unpublished data), the NK Flt3ITD$^+$ samples had very high *meis1* and *c-jun* expression (Fig. 2). However, there was a significant suppression of *DAPK1* transcripts (Fig. 2A). In most of the examples noted above, *DAPK1* levels were 10- to 100-fold lower than in the controls, when normalized to *c*-Jun (Fig. 2A). In fact, a statistically significant difference in *DAPK1*/*c-jun* expression was noted when we compared the populations with NKFlt3ITD [or tMLL; as a positive-control for *DAPK1* repression; ref. 19] to AMLs having other cytogenetic/genotypic profiles, where

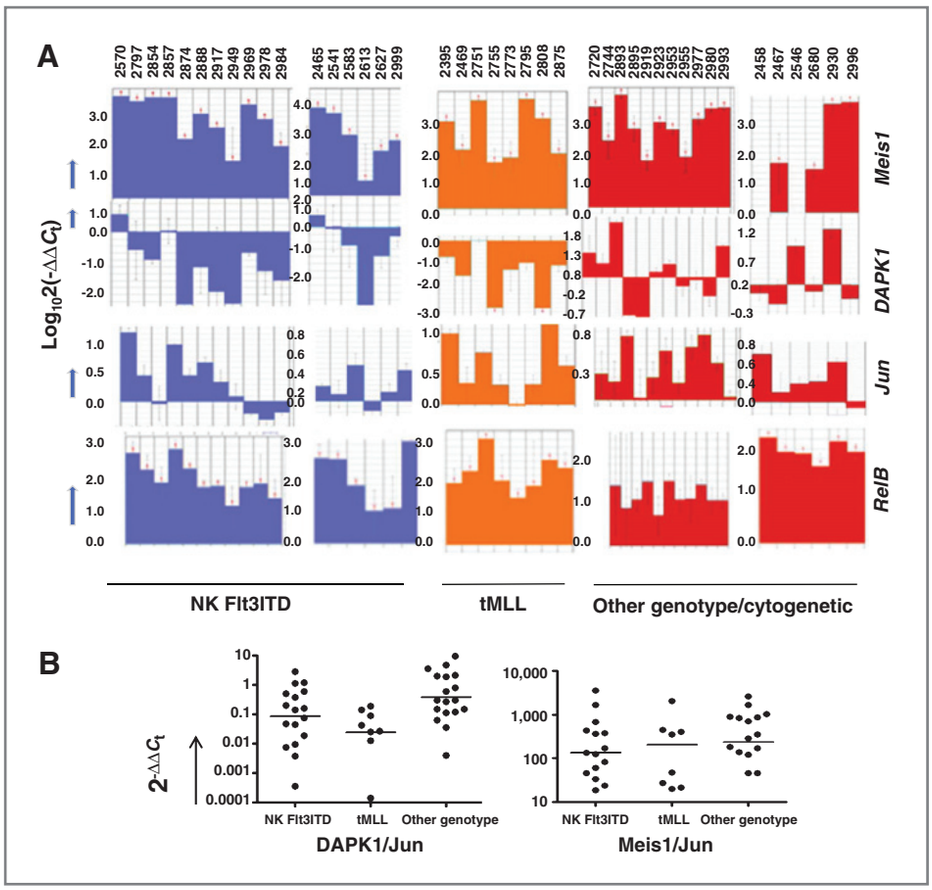

Figure 2. A dichotomy exists in *Meis1*, *c-jun*, and *relB* expression (which are known to be *c*-Jun–dependent) versus *DAPK1* (the dually responsive *c*-Jun/NF-κB–dependent gene) in patient groups with normal karyotype Flt3ITD or MLL translocation. A, expression levels of *DAPK1* are significantly different in NK Flt3ITD or MLL translocation AMLs when compared with cases without Flt3ITD or nonrandom cytogenetic abnormalities. B, in normal karyotype Flt3ITD and the tMLL AML groups, the expression ratios of DAPK1 to *c*-Jun were statistically less than other cytogenetic/genotype categories, but there was no difference in the ratios of *Meis1* to *c-jun*.

differences in *Meis1*/*c-jun* levels were not significantly different (Fig. 2B; *DAPK1*/*c-jun*: Mann–Whitney/Wilcoxon one-sided test: NKFlt3ITD or tMLL vs. other cytogenetic/genotype groups: $P < 0.041$ or $P < 0.0006$, respectively; *Meis1*/*c-jun* = not statistically significant). *RelB*, which is partially *c*-Jun-responsive (26), was uniformly highly expressed (Fig. 2A).

Therefore, Flt3ITD$^+$ MV-4-11 cell line was used as a model to further explore the relationship between Flt3, TAK1, and JNK1/phospho-c-jun versus IKK/NF-κB (Fig. 3). We first knocked down Flt3 using RNAi. Flt3 knockdown (78%) resulted in a significant loss of TAK1 phosphorylation (53%; Fig. 3A). [We previously showed that Flt3 knockdown leads to a loss of JNK activity and *c*-Jun phosphorylation (Fig. 1C; ref. 9)]. Indeed, RNAi-mediated knockdown of either JNK1 or TAK1 also suppressed the expression of phosphorylated *c*-Jun, by 100% or 80%, respectively (Fig. 3B). In addition, we found that TAK1-inactivation essentially led to total loss/destabilization of NIK (Fig. 3A). NIK is a MAP3K required for noncanonical NF-κB activation but sensitive to TAK1 activation-dependent stabilization (28). Thus, loss of Flt3 would be expected to affect activation of either canonical NF-κB (solely involving TAK1) or noncanonical NF-κB (TAK1/NIK; Fig. 3A; and see below).

To study the activation status of NF-κB species, cellular lysates were fractionated into cytoplasmic and nuclear components because nuclear retention of these proteins determines their transcriptional activity. We and others have shown that phosphorylated *c*-Jun (at S^{63}, S^{73}) is always predominantly present in the nucleus as a heterodimer with other proteins (refs. 9, 29). Surprisingly, we found that, in MV-4-11 cells, p65 NF-κB was largely absent in the nuclear fraction, although an abundant quantity of Sp1 (a constitutively nuclear transcription factor), but not GAPDH (a cytoplasmic marker), was found (Fig. 3C). Furthermore, the RNAi-mediated knockdown of Flt3, TAK1, NIK, and JNK1 failed to increase nuclear levels of p65NF-κB (Fig. 3C).

In contrast, control MV-4-11 (Fig. 3C) had ∼50% fraction of p52NF-κB in the nucleus, and a lesser amount of relB, (a primary heterodimeric partner of p52NF-κB; Fig. 3C). Knockdown of either TAK1 or NIK strongly decreased nuclear p52NF-κB levels by 73% or 76%, respectively, with a corresponding increase in cytoplasmic levels (Fig. 3C, panel 1; and see below). Knockdown of JNK1 or Flt3 appeared to diminish overall cytoplasmic and nuclear content of both relB and p52NF-κB by 76% and 50%, respectively (Fig. 3C, panels 1 and 2). This is consistent with stability of this heterodimeric complex relying on partner relB, whose expression is induced by *c*-Jun (Fig. 3C; ref. 26). Taken together, our data support the existence of an Flt3–p52NF-κB pathway, which may negatively regulate *DAPK1* expression (Figs. 1–3).

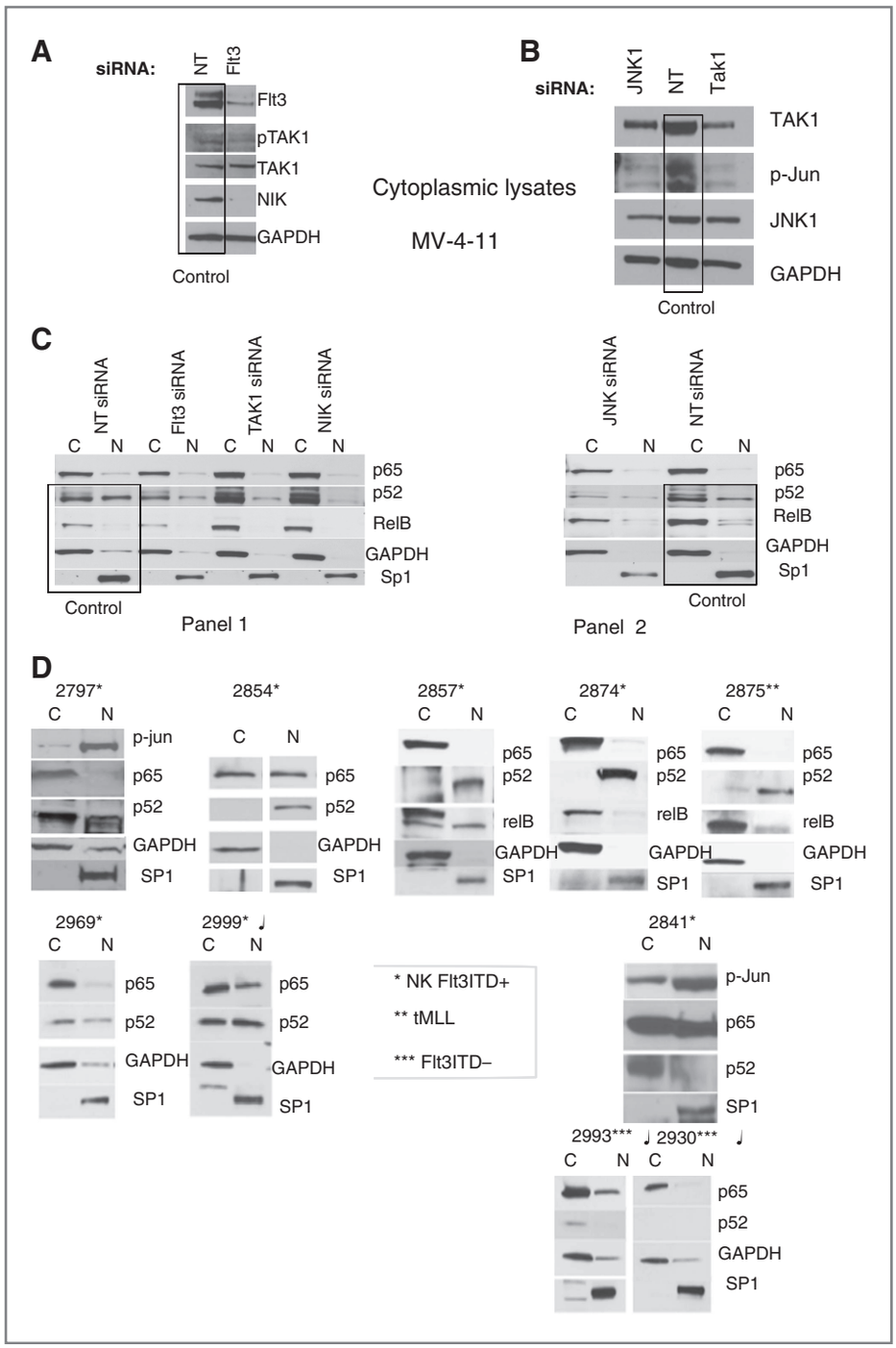

Figure 3. In Flt3ITD$^+$ AMLs, the Flt3-to-TAK1 pathway is involved in establishing an effector apparatus involving p52NF-κB for DAPK1 repression, whereas primary Flt3ITD$^-$ AMLs with high DAPK1 expression lack nuclear p52NF-κB. Flt3 knockdown blocked TAK1-activating phosphorylation (78% and 53% by densitometry, respectively) and led to NIK degradation, which inhibits the activation of noncanonical NF-κB (A). B, JNK1 and TAK1 knockdown lead to diminution of *c*-Jun phosphorylation by 100% and 80%, respectively. C, control MV-4-11 cells (NT siRNA ×2), nuclear fraction is characterized by dominant expression levels of p52NF-κB and relB, but not p65NF-κB. Flt3, TAK1, or NIK knockdown lead to diminution of nuclear (N) p52NF-κB levels (by 46%, 73%, or 76%, respectively; Panel 1). JNK1 knockdown led to diminution of p52NF-κB levels (by 76%; Panel 2). In addition, Flt3 knockdown reduced overall p52NF-κB levels (by 50%; Panel 1). D, nuclear translocation of p52NF-κB is dominant among NKFlt3ITD$^+$ AML with DAPK1 repression (#2797, 49%; #2854, 100%; #2857, 70%; #2874, 100%; #2969, 35%; #2999, 50%). Note that the ITD$^+$ sample #2999 was exposed on the same blot with ITD$^-$ #2993 and 2930, with no nuclear p52NF-κB). C, cytoplasm; NT, nontargeting.

As three fourths of primary Flt3ITD$^+$ AML cases presented in Fig. 1B were refractory to primary treatment (all except #2841) and had low DAPK1 expression, we hypothesized that this pathway might have a biologic/prognostic significance. Indeed, sample #2841 with high DAPK1 expression differed greatly from 7 other Flt3ITD$^+$ samples and a control tMLL AML because it had trivial amounts of nuclear p52NF-κB and abundant and predominantly nuclear p65NF-κB (Fig. 3D; and see below). These NKFlt3ITD$^+$ AMLs with little or no *DAPK1* expression, as in the control tMLL AML, were distinguished by predominantly nuclear p52NF-κB (mean% nuclear translocation p52NF-κB, 72.8 ± 9.9%; vs. mean% nuclear translocation p65NF-κB, 19.6 ± 6.6%). In fact, qPCR analysis showed very low *DAPK1* transcripts among samples with no nuclear p65, for example, 2797, 2874, and 2857 (compare Fig. 3D with Fig. 2A). On

the other hand, the higher and dominant content of nuclear p65NF-κB in #2841 was more typical of the above-mentioned Flt3ITD$^-$ patients—where DAPK1 levels were high, and had little or no nuclear p52NF-κB (#2930, 2993 in Figs. 1, 2, and 3D). In addition, the dominant nuclear presence for p52NF-κB compared with p65NF-κB in the different cohorts was confirmed by gel mobility-shift assays in addition to immunoblotting (Supplementary Fig. S1). We ascertained that the isolation procedure/washing had not created artifactual deficiency of nuclear p65NF-κB (on any potential autocrine cytokine washout) by carrying out timed re-additions to cultured AML blasts of Flt3 ligand (ref. 30; data not shown).

p52NF-κB and HDAC repress *DAPK1* transcription in MV-4-11 and primary AML blasts with Flt3ITD or MLL translocation

We next investigated a possible Flt3ITD-driven mechanism that linked p52NF-κB to *DAPK1* repression in MV-4-11. Because HDACs are known to cause gene repression, we next determined whether p52 NF-κB, *c*-Jun, and HDAC would bind to the *DAPK1* promoter. ChIP assays revealed a strong binding of both p52NF-κB and HDAC2 to the *DAPK1* promoter (Fig. 4). In contrast, a relatively weaker binding of *c*-Jun and HDAC1 to *DAPK1* promoter was observed, when compared with HDAC2 (Fig. 4A). In another series of ChIP experiments, we found that, among HDACs, strong binding of the HDAC2 (class I) to the promoter accompanied a corresponding absence of HDAC-5 (class II) and class IV HDAC11, which have been found to be predominantly localized to cytoplasm in certain hematopoietic cells and are expressed low in MV-4-11 (Fig. 4B). On the other hand, a moderate binding of the class II HDAC6 occurred. The latter has a nuclear localization signal and has been found to shuttle between nucleus (e.g., in association with *c*-Jun/CREB/RUNX2/steroid receptors on chromatin) and cytoplasm for functions. In the cytoplasm, a dominant role for HDAC6 in regulating hsp90 chaperone function has been noted in AML cell lines as well (Fig. 4B; refs. 31–36).

To provide additional evidence for a role of p52NF-κB in repressing *DAPK1*, knockdown experiments in MV-4-11 cells were undertaken (Fig. 4C–E). RNAi-mediated knockdown of p52NF-κB, or its upstream activator NIK, caused an increase in DAPK1 protein expression by 2-fold (Fig. 4C and D). As expected, knockdown of either JNK1 or Flt3 in

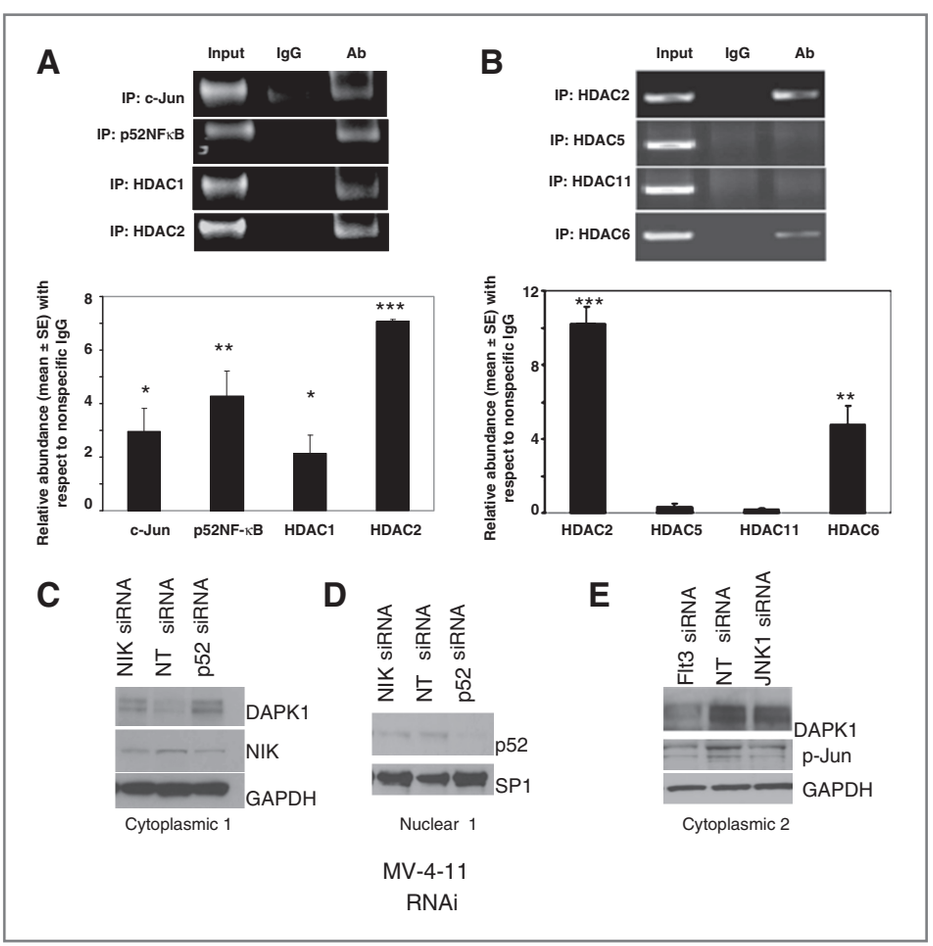

Figure 4. ChIP analyses have shown that the tandem CRE and NF-κB sites of the proximal *DAPK1* promoter are occupied by *c*-Jun and, to a greater extent, by p52NF-κB and HDAC2. A and B, typical PCR patterns obtained in ChIP assays with *DAPK1*-specific primers in MV-4-11 cells are shown. For input-control reactions, one fifth of the soluble chromatin used for the ChIP analysis was used. In each case, 30 cycles of PCR were carried out. Nonspecific IgG, HDAC1, HDAC2, p52 NFκB, and *c*-Jun, as well as HDAC5, HDAC11, and HDAC6 IgGs were used at concentration of 5 μg each per reaction. Real-time PCR analysis of *DAPK1* promoter fragments recovered in ChIP assays conducted with the indicated antibodies. Each bar represents the mean abundance of *DAPK1* promoter fragments for specific antibody when compared with nonspecific IgG. SE of 6 separate reactions from 2 independent experiments are shown. ***, $P < 0.001$; **, $P < 0.01$; *, $P < 0.05$. RNAi-mediated knockdown of p52NF-κB or NIK (C and D) upregulated DAPK1 expression. Flt3 or JNK1 knockdown reduce phospho–*c*-Jun and DAPK1 levels by 60% and 40%, respectively (C–E). IP, immunoprecipitation; NT, nontargeting.

MV-4-11 downregulated *DAPK1* levels by 40% or 60%, respectively (Fig. 4E), similar to the data shown in Fig. 1C. Therefore, *DAPK1* was de-repressed following the knockdown of p52NF-κB when JNK1 arm of Flt3 signaling was sustained (Fig. 4). In addition, the identification of severe *DAPK1* repression (Figs. 2 and 3D) is consistent with the relationship between p52NF-κB and *DAPK1* in MV-4-11.

Discussion

Genome-wide sequencing studies to identify gene mutations among the majority of solid tumors can be compared with similar screens carried out with AML. Such comparison indicates that the mutational complexity of adult AML is modest and may involve 10- to 300-fold lower numbers of mutated genes (37–42). In the case of normal karyotype AMLs with Flt3ITD mutation, only 10 to 14 genes have been found mutated and the important founder mutations appear to involve not only the *Flt3* and *NPM1* genes, but also epigenetically active enzymes (39–42). Perhaps because of the involvement of intrinsic epigenetic mechanisms in many examples of the heterogenous disease process, clinical use of single-agent Flt3-selective tyrosine kinase inhibitors has not showed truly significant disease-free survival in most patients with Flt3ITD$^+$ AML.

As the epigenetic signature of AMLs is robust, particularly in the setting of *Flt3ITD* mutation (41–43), we postulated that the unique signaling pathway used by Flt3ITD may contribute to those "stress-induced" steps involved in epigenetic reprogramming in Flt3ITD$^+$ AMLs (12, 17, 18). We further postulated that TAK1, which is overexpressed in a poor-risk AML LSC signature (22), may contribute to p52NF-κB–induced epigenetic silencing, similar to the ability for Evi-1 to attract a *cis*-localized epigenetic apparatus to distinct genes in an AML subgroup (44). Indeed, our data point to the existence of an instructive mechanism (as opposed to a "stochastic" origin) for transcriptional repression of certain tumor suppressor genes, as shown here for *DAPK1*. *DAPK1* is regulated by a binary *cis*-element consisting of CRE/Jun and κB sites (12, 13). These sites are subject to dominant-negative regulation by p52NF-κB and HDAC2/HDAC6 under the Flt3-/TAK1 pathway (Figs. 3–5). Inhibition of p52NF-κB caused a de-repression of *DAPK1*.

Very little is known about the role of p52NF-κB as a regulator of gene expression in AML (45). In one study, epigenetic repression of another tumor suppressor gene, DIF2 was indirectly linked to the activity of p52NF-κB. In addition, there has been inadequate explanation for the severe reduction of *DAPK1* expression in poor-risk AML. In fact, previous studies have identified much lower levels of *DAPK*1 promoter hypermethylation than would have been expected of the observed extent of transcriptional repression in AML (16, 41–43, 46, 47). This is in contrast to MLL-r infant ALL, where the DAPK1 repression was associated with its promoter hypermethylation (19). In this study, we showed that, for the subset of AMLs characterized by Flt3ITD, often with additional NPM1 and/or IDH1/2 or DNMT3 mutation, upstream signals may provide the stimulus for p52NF-κB, and its partner relB, to attract HDACs and possibly other repressors to specific gene promoters to enforce a repression (12, 47).

The Flt3-/TAK1-dependent activation of IKK's/NF-κB and JNK1 that we identified in this study is pertinent to activation of these latter 2 crucial downstream tumor effectors. In addition, TAK1 may bear upon other antiapoptotic participants, including AMP kinase, which is activated by TAK1 for additional antiapoptotic function in the TRAIL pathway (48, 49). Although TAK1 has more frequently been associated with the canonical NF-κB pathway rather than the NIK-dependent noncanonical pathway we identified, there is ample precedent that TAK1 can activate NIK, and that TAK1/TRAF6-ubiquitin conjugates activate IKKα as well as IKKβ (28, 50).

Furthermore, the data we report has implications for the design of a mechanistically driven therapeutic regimen-to inhibit Flt3ITD$^+$ AML. DAPK1 suppression in context of Flt3ITD activation of p52NF-κB implies that 1 criterion for selection of tyrosine kinase inhibitors, classified as Flt3 inhibitors, is in their ability to inhibit p52NF-κB activation in this subgroup of AMLs. In turn, HDAC inhibitors contribute independently toward *DAPK1* de-repression for its participation in ER stress apoptosis. Bortezomib is also known to inhibit steps required for proteasomal activation of p52NF-κB (51) This indicates a synergistic potential for combining these drug classes in "targeted" therapy of Flt3ITD$^+$ AML (Fig. 5). Indeed, we have both *in vitro* and *in vivo* evidence that such an approach may enforce apoptosis via enhanced ER stress following *DAPK1* de-repression in

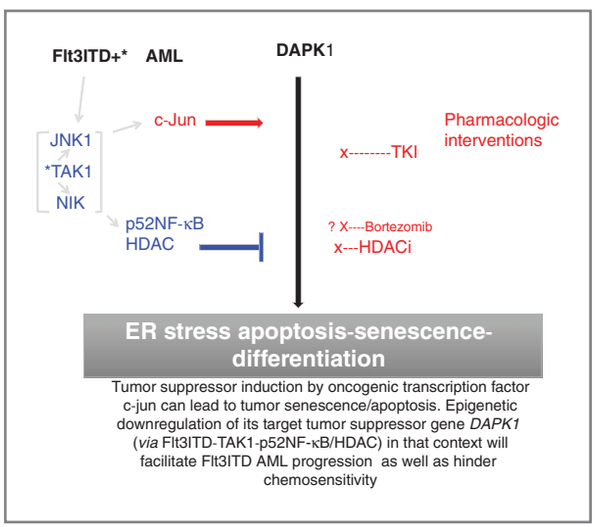

Figure 5. A model for the repression of DAPK1 by Flt3ITD-induced signals. Although c-Jun elicited by Flt3ITD/JNK1 drives *DAPK1* transcription, this activity is blocked by p52NF-κB which recruits HDAC2/HDAC6. De-repression of *DAPK1* can be achieved by use of a TKI/Flt3 inhibitor, particularly in combination with an HDAC inhibitor (e.g., SAHA/vorinostat) and/or bortezomib as a proteasomal inhibitor of p52NF-κB φιγ. HDACi, HDAC inhibitor; TKI, tyrosine kinase inhibitor.

association with p52NF-κB depletion by the combination of a Flt3 inhibitor and an HDAC inhibitor in Flt3ITD$^+$ AML (H Sayar et al., manuscript in preparation).

Finally, the enzymatic activity of the co-oncogene peptidyl prolylisomerase 1 (PIN1), required for tyrosine kinase-mediated JNK/*c*-Jun signaling in breast cancer and AML, is abrogated by DAPK1-mediated phosphorylation on serine 71 of PIN1 (52–54). Thus, the pathophysiologic significance of *DAPK1* repression in these malignancies is further emphasized, along with the therapeutic strategy for combining tyrosine kinase and HDAC inhibitors.

Disclosure of Potential Conflicts of Interests

No potential conflicts of interest were disclosed.

Authors' Contributions

R. Shanmugam and P. Gade planned and carried out experiments, analyzed results, and wrote the manuscript. A. Wilson-Weekes planned and carried out experiments and analyzed results. S. Gupta planned and carried out experiments. H. Sayar screened patients and edited the manuscript. A. Suvannasankha analyzed results and edited the manuscript. C. Goswami, L. Li, A.A. Cardoso, and T. Al Baghdadi analyzed results and reviewed the manuscript. K.J. Sargent and L.D. Cripe screened patients and reviewed the manuscript. D.V. Kalvakolanu planned experiments, analyzed results, and wrote the manuscript. H.S. Boswell designed the study, planned and carried out experiments, analyzed results, and wrote the manuscript.

Grant Support

This work was supported in part by the Department of Veterans Affairs Merit Review Award (H.S. Boswell), and stipend in memory of Dr. Gary D. Tollefson. D.V. Kalvakolanu is supported by NIH grant CA78282.

The costs of publication of this article were defrayed in part by the payment of page charges. This article must therefore be hereby marked *advertisement* in accordance with 18 U.S.C. Section 1734 solely to indicate this fact.

Received November 12, 2010; revised October 7, 2011; accepted November 1, 2011; published OnlineFirst November 17, 2011.

References

1. Schardt JA, Weber D, Eyholzer M, Mueller BU, Pabst T. Activation of the unfolded protein response is associated with favorable prognosis in acute myeloid leukemia. Clin Cancer Res 2009;15:3834–41.
2. Choudhary C, Olsen JV, Brandts C, Cox J, Reddy PN, Böhmer FD, et al. Mislocalized activation of oncogenic RTKs switches downstream signaling outcomes. Mol Cell 2009;36:326–39.
3. Rahmani M, Davis EM, Crabtree TR, Habibi JR, Nguyen TK, Dent P, et al. The kinase inhibitor sorafenib induces cell death through a process involving induction of endoplasmic reticulum stress. Mol Cell Biol 2007;27:5499–513.
4. Szegezdi E, Macdonald DC, Ní Chonghaile T, Gupta S, Samali A. Bcl-2 family on guard at the ER. Am J Physiol Cell Physiol 2009;296: C941–53.
5. Chang NC, Nguyen M, Germain M, Shore GC. Antagonism of Beclin 1-dependent autophagy by Bcl-2 at the endoplasmic reticulum requires NAF-1. EMBO J 2010;29:606–18.
6. Kim I, Xu W, Reed JC. Cell death and endoplasmic reticulum stress: disease relevance and therapeutic opportunities. Nat Rev Drug Discov 2008;7:1013–30.
7. Bialik S, Kimchi A. The death-associated protein kinases: structure, function, and beyond. Ann Rev Biochem 2006;75:189–210.
8. Martioriati A, Doumont G, Alcalay M, Bellefroid E, Pelicci PG, Marine JC, et al. *dapk1,* encoding an activator of p19arf-p53-mediated apoptotic checkpoint, is a transcriptional target of p53. Oncogene 2005;24:1461–6.
9. Hartman AD, Wilson-Weekes A, Suvannasankha A, Burgess GS, Phillips CA, Hincher KJ, et al. Constitutive c-jun N-terminal kinase activity in acute myeloid leukemia derives from Flt3 and affects survival and proliferation. Exp Hematol 2006;34:1360–76.
10. Hess P, Pihan G, Sawyers CL, Flavell RA, Davis RJ. Survival signaling mediated by c-Jun NH(2)-terminal kinase in transformed B lymphoblasts. Nat Genet 2002;32:201–5.
11. Hayakawa J, Mittal S, Wang Y, Korkmaz KS, Adamson E, English C, et al. Identification of promoters bound by c-Jun/ATF2 during rapid large-scale gene activation following genotoxic stress. Mol Cell 2004;16:521–35.
12. Puto LA, Reed JC. Daxx represses RelB target promoters via DNA methyltransferase recruitment and DNA hypermethylation. Genes Dev 2008;22:998–1010.
13. Gade P, Roy SK, Li H, Nallar SC, Kalvakolanu DV. Critical role for transcription factor C/EBP-beta in regulating the expression of death-associated protein kinase 1. Mol Cell Biol 2008;28:2528–48.
14. Huang W, Ghisletti S, Perissi V, Rosenfeld MG, Glass CK. Transcriptional integration of TLR2 and TLR4 signaling at the NCoR derepression checkpoint. Mol Cell 2009;35:48–57.
15. Guzman ML, Upchurch D, Grimes B, Howard DS, Rizzieri DA, Luger SM, et al. Expression of tumor-suppressor genes interferon regulatory factor 1 and death-associated protein kinase in primitive acute myelogenous leukemia cells. Blood 2001;97:2177–9.
16. Fandy TE, Herman JG, Kerns P, Jiemjit A, Sugar EA, Choi SH, et al. Early epigenetic changes and DNA damage do not predict clinical response in an overlapping schedule of 5-azacytidine and entinostat in patients with myeloid malignancies. Blood 2009;114:2764–73.
17. Johnstone SE, Baylin SB. Stress and the epigenetic landscape: a link to the pathobiology of human diseases? Nat Rev Genet 2010;11: 806–12.
18. Gazin C, Wajapeyee N, Gobeil S, Virbasius CM, Green MR. An elaborate pathway required for Ras-mediated epigenetic silencing. Nature 2007;449:1073–7.
19. Schafer E, Irizarry R, Negi S, McIntyre E, Small D, Figueroa ME, et al. Promoter hypermethylation in MLL-r infant acute lymphoblastic leukemia: biology and therapeutic targeting. Blood 2010;115: 4798–809.
20. Schlenk RF, Döhner K, Krauter J, Fröhling S, Corbacioglu A, Bullinger L, et al. German–Austrian Acute Myeloid Leukemia Study Group. Mutations and treatment outcome in cytogenetically normal acute myeloid leukemia. N Engl J Med 2008;358:1909–18.
21. Sanna MG, da Silva Correia J, Ducrey O, Lee J, Nomoto K, Schrantz N, et al. IAP suppression of apoptosis involves distinct mechanisms: the TAK1/JNK1 signaling cascade and caspase inhibition. Mol Cell Biol 2002;22:1754–66.
22. Eppert K, Takenaka K, Lechman ER, Waldron L, Nilsson B, van Galen P, et al. Stem cell gene expression programs influence clinical outcome in human leukemia. Nat Med 2011;17:1086–93.
23. Valk PJ, Verhaak RG, Beijen MA, Erpelinck CA, Barjesteh van Waalwijk van Doorn-Khosrovani S, Boer JM, et al. Prognostically useful gene-expression profiles in acute myeloid leukemia. N Engl J Med 2004;350:1617–28.
24. Livak KJ, Schmittgen TD. Analysis of relative gene expression data using real-time quantitative PCR and the 2(-Delta Delta C(T)) method. Methods 2001;25:402–8.
25. Wilson BE, Mochon E, Boxer LM. Induction of bcl-2 expression by phosphorylated CREB proteins during B cell activation and rescue from apoptosis. Mol Cell Biol 1996;16:5546–56.

26. Mineva ND, Rothstein TL, Meyers JA, Lerner A, Sonenshein GE. CD40 ligand-mediated activation of the de novo RelB NF-kappaB synthesis pathway in transformed B cells promotes rescue from apoptosis. J Biol Chem 2007;282:17475–85.

27. Compagno M, Lim WK, Grunn A, Nandula SV, Brahmachary M, Shen Q, et al. Mutations of multiple genes cause deregulation of NF-kappaB in diffuse large B-cell lymphoma. Nature 2009;459:717–21.

28. Ninomiya-Tsuji J, Kishimoto K, Hiyama A, Inoue J, Cao Z, Matsumoto K. The kinase TAK1 can activate the NIK-I kappaB as well as the MAP kinase cascade in the IL-1 signalling pathway. Nature 1999;398:252–6.

29. Liu H, Deng X, Shyu YJ, Li JJ, Taparowsky EJ, Hu CD. Mutual regulation of c-Jun and ATF2 by transcriptional activation and subcellular localization. EMBO J 2006;25:1058–69.

30. Ludwig D, Hicklin D, Witte L, Li Y, Small D. FLT3 ligand causes autocrine signaling in acute myeloid leukemia cells. Blood 2004;103: 267–74.

31. Keedy KS, Archin NM, Gates AT, Espeseth A, Hazuda DJ, Margolis DM. A limited group of class I histone deacetylases acts to repress human immunodeficiency virus type 1 expression. J Virol 2009;83: 4749–56.

32. Bradbury CA, Khanim FL, Hayden R, Bunce CM, White DA, Drayson MT, et al. Histone deacetylases in acute myeloid leukaemia show a distinctive pattern of expression that changes selectively in response to deacetylase inhibitors. Leukemia 2005;19:1751–9.

33. Xu X, Xie C, Edwards H, Zhou H, Buck SA, Ge Y. Inhibition of histone deacetylases 1 and 6 enhances cytarabine-induced apoptosis in pediatric acute myeloid leukemia cells. PLoS One 2011;6: e17138.

34. Govindan MV. Recruitment of cAMP-response element-binding protein and histone deacetylase has opposite effects on glucocorticoid receptor gene transcription. J Biol Chem 2010;285: 4489–510.

35. Westendorf JJ, Zaidi SK, Cascino JE, Kahler R, van Wijnen AJ, Lian JB, et al. Runx2 (Cbfa1, AML-3) interacts with histone deacetylase 6 and represses the p21(CIP1/WAF1) promoter. Mol Cell Biol 2002;22: 7982–92.

36. Bali P, Pranpat M, Bradner J, Balasis M, Fiskus W, Guo F, et al. Inhibition of histone deacetylase 6 acetylates and disrupts the chaperone function of heat shock protein 90: a novel basis for antileukemia activity of histone deacetylase inhibitors. J Biol Chem 2005;280: 26729–34.

37. Pleasance ED, Cheetham RK, Stephens PJ, McBride DJ, Humphray SJ, Greenman CD, et al. A comprehensive catalogue of somatic mutations from a human cancer genome. Nature 2010;463:191–6.

38. Pleasance ED, Stephens PJ, O'Meara S, McBride DJ, Meynert A, Jones D, et al. A small-cell lung cancer genome with complex signatures of tobacco exposure. Nature 2010;463:184–90.

39. Ley TJ, Mardis ER, Ding L, Fulton B, McLellan MD, Chen K, et al. DNA sequencing of a cytogenetically normal acute myeloid leukaemia genome. Nature 2008;456:66–72.

40. Mardis ER, Ding L, Dooling DJ, Larson DE, McLellan MD, Chen K, et al. Recurring mutations found by sequencing an acute myeloid leukemia genome. N Engl J Med 2009;361:1058–66.

41. Ley TJ, Ding L, Walter MJ, McLellan MD, Lamprecht T, Larson DE, et al. DNMT3A mutations in acute myeloid leukemia. N Engl J Med 2010; 363:2424–33.

42. Figureroa ME, Abel-Wahab O, Lu C, Ward PS, Patel J, Shih A, et al. Leukemic IDH1 and IDH2 mutations result in a hypermethylation phenotype, disrupt TET2 function, and impair hematopoietic differentiation. Cancer Cell 2010;18:553–67.

43. Figueroa ME, Lugthart S, Li Y, Erpelinck-Verschueren C, Deng X, Christos PJ, et al. DNA methylation signatures identify biologically distinct subtypes in acute myeloid leukemia. Cancer Cell 2010;17: 13–27.

44. Lugthart S, Figueroa ME, Bindels E, Skrabanek L, Valk PJ, Li Y, et al. Aberrant DNA hypermethylation signature in acute myeloid leukemia directed by EVI1. Blood 2011;117:234–41.

45. Laurenzana A, Petruccelli LA, Pettersson F, Figueroa ME, Melnick A, Baldwin AS, et al. Inhibition of DNA methyltransferase activates tumor necrosis factor alpha-induced monocytic differentiation in acute myeloid leukemia cells. Cancer Res 2009;69:55–64.

46. Claus R, Hackanson B, Poetsch AR, Zucknick M, Sonnet M, Blagitko-Dorfs N, et al. Quantitative analyses of DAPK1 methylation in AML and MDS. Int J Cancer 2011 Sep 14. [Epub ahead of print].

47. Cedar H, Bergmann Y. Linking DNA methylation and histone modification: patterns and paradigms. Nat Rev Genet 2009;10:295–304.

48. Morioka S, Omori E, Kajino T, Kajino-Sakamoto R, Matsumoto K, Ninomiya-Tsuji J. TAK1 kinase determines TRAIL sensitivity by modulating reactive oxygen species and cIAP. Oncogene 2009;28: 2257–65.

49. Herrero-Martín G, Høyer-Hansen M, García-García C, Fumarola C, Farkas T, López-Rivas A, et al. TAK1 activates AMPK-dependent cytoprotective autophagy in TRAIL-treated epithelial cells. EMBO J 2009;28:677–85.

50. Xia ZP, Sun L, Chen X, Pineda G, Jiang X, Adhikari A, et al. Direct activation of protein kinases by unanchored polyubiquitin chains. Nature 2009;461:114–9.

51. Skaug B, Jiang X, Chen ZJ. The role of ubiquitin in NF-kappaB regulatory pathways. Annu Rev Biochem 2009;78:769–96.

52. Wulf GM, Ryo A, Wulf GG, Lee SW, Niu T, Petkova V, et al. Pin1 is overexpressed in breast cancer and cooperates with Ras signaling in increasing the transcriptional activity of c-Jun towards cyclin D1. EMBO J 2001;20:3459–72.

53. Pulikkan JA, Dengler V, Peer Zada AA, Kawasaki A, Geletu M, Pasalic Z, et al. Elevated PIN1 expression by C/EBPalpha-p30 blocks C/EBP alpha-induced granulocytic differentiation through c-Jun in AML. Leukemia 2010;24:914–23.

54. Lee TH, Chen CH, Suizu F, Huang P, Schiene-Fischer C, Daum S, et al. Death-associated protein kinase 1 phosphorylates Pin1 and inhibits its prolyl isomerase activity and cellular function. Mol Cell 2011;42: 147–59.